CHEMISTRY OF MATERIALS
Article

Chem. Mater. **2010,** *22,* 3875–3883 3875
DOI:10.1021/cm903713q

Inkjet-Printing-Engineered Functional Microdot Arrays Made of Mesoporous Hybrid Organosilicas

Bruno Fousseret,[†] Marion Mougenot,[†] Fabrice Rossignol,[†] Jean-François Baumard,[†] Bernard Soulestin,[†] Cédric Boissière,[‡] François Ribot,[‡] Dominique Jalabert,[§] Claire Carrion,[⊥] Clément Sanchez,[‡] and Martine Lejeune*,[†]

[†]*Laboratoire de Science des Procédés Céramiques et de Traitements de Surface, UMR CNRS 6638, Ecole Nationale Supérieure de Céramique Industrielle, 47−73 avenue Albert Thomas, 87065 Limoges, France,* [‡]*Laboratoire de Chimie de la Matière Condensée de Paris, UMR CNRS 7574, Université Pierre et Marie Curie Paris VI, Collège de France, 11 place Marcelin Berthelot, 75231 Paris Cedex 05, France,* [§]*Centre de Microscopie Electronique, Faculté des Sciences et Techniques, Université d'Orléans, 1 rue de Chartres, 45067 Orléans Cedex, France, and* [⊥]*Plateforme Cytométrie-Imagerie-Mathématiques, UMR CNRS 6101, Faculté de médecine, 2 rue du Dr Marcland, 87025 Limoges Cedex, France*

Received December 10, 2009. Revised Manuscript Received May 19, 2010

The fabrication of three-dimensional fine-scale microdot arrays of organized mesoporous hybrid organosilicas by the coupling of inkjet printing (IJP) and Pluronic F127 driven evaporation-induced self-assembly (EISA) in the presence of cocondensed silica and organosilica precursors is demonstrated. The mesoorganization can be optimized by tuning both processing and chemical parameters (the drying time between successive layers, droplet volume, chemical composition, temperature, and aging time of the colloidal sol). The feasibility of one-pot multifunctionalization with both TFTS $CF_3(CF_2)_5CH_2CH_2Si(OC_2H_5)_3$ and thiol functionalities $HSCH_2CH_2CH_2Si(OC_2H_5)_3$ is also demonstrated, emphasizing the wide range of accessible nanostructured porous hybrid materials that result from the coupling of IJP and EISA. From this demonstrative concept, many hybrid materials with applications in the field of multiarray sensors and smart membranes can be expected. Moreover, the peculiar role of the hydrophobic organosilane TFTS $CF_3(CF_2)_5CH_2CH_2Si(OC_2H_5)_3$, as promoter of the structural mesoorganization of hybrid microdots, is discussed. The hydrophobic nature of microdot arrays is characterized as a function of TFTS addition and surface morphology. Tuning both the amount of the hydrophobic component and microdot-induced surface patterning allows controlled one-pot synthesis of hyperhydrophobic surfaces with contact angles rising up to 131°. Moreover, the possibility of grafting via *one-pot* synthesis a thiol function, allowing the trapping of gold nanoparticles, is demonstrated.

Introduction

The ability to create "organized matter" at the micro-, meso-, and nanoscales has been a significant breakthrough[1,2] since the discovery that micellar and lyotropic liquid-crystal phases can act as templates for the designed synthesis of periodically organized mesoporous materials.[3−7] In the past few years, an increasing quantity of mesostructured and mesoporous materials with very diverse chemical compositions (oxides, metals, carbons, chalcogenides, semiconductors, etc.) shaped as powders, monoliths, thin films, membranes, or fibers have appeared.[8,9] These materials can be processed using several approaches, among them true or evaporation-induced liquid-crystal templating and nanocasting.[8,10]

In the past decade, numerous works have been reported on the fabrication of mesoporous silica films by evaporation-induced self-assembly (EISA); i.e., by preferential evaporation of a solution of polymerizable inorganic precursors and surfactant molecules,[9,11] a cooperative self-assembly occurs. During EISA, amphiphilic molecules or amphiphilic block copolymers and inorganic species combine in a first step to form hybrid intermediate entities

*To whom correspondence should be addressed. Tel: +33 5 55 45 22 27. Fax: +33 5 55 79 09 98. E-mail: martine.lejeune@unilim.fr.

(1) Kresge, C. T.; Leonowicz, M. E.; Roth, W. J.; Vartuli, J. C.; Beck, J. S. *Nature* **1992**, *359*(6397), 710–712.
(2) Beck, J. S.; Vartuli, J. C.; Roth, W. J.; Leonowicz, M. E.; Kresge, C. T.; Schmitt, K. D.; Chu, C. T. W.; Olson, D. H.; Sheppard, E. W.; McCullen, S. B.; Higgins, J. B.; Schlenker, J. L. *J. Am. Chem. Soc.* **1992**, *114*(27), 10834–10843.
(3) Ozin, G. A. *Chem. Commun.* **2000**, *6*, 419–432.
(4) Antonietti, M.; Ozin, G. A. *Chem.—Eur. J.* **2004**, *10*(1), 28–41.
(5) Antonietti, M.; Berton, B.; Göltner, C.; Hentze, H. P. *Adv. Mater.* **1998**, *10*(2), 154–159.
(6) Mann, S.; Burkett, S. L.; Davis, S. A.; Fowler, C. E.; Mendelson, N. H.; Sims, S. D.; Walsh, D.; Whilton, N. T. *Chem. Mater.* **1997**, *9* (11), 2300–2310.
(7) Zhao, D.; Feng, J.; Huo, Q.; Melosh, N.; Fredrickson, G. H.; Chmelka, B. F.; Stucky, G. D. *Science* **1998**, *279*(5350), 548–552.
(8) Soler-Illia, G. J. D. A. A.; Sanchez, C.; Lebeau, B.; Patarin, J. *Chem. Rev.* **2002**, *102*(11), 4093–4138.
(9) Sanchez, C.; Boissière, C.; Grosso, D.; Laberty, C.; Nicole, L. *Chem. Mater.* **2008**, *20*(3), 682–737.
(10) Attard, G. S.; Bartlett, P. N.; Coleman, N. R. B.; Elliott, J. M.; Owen, J. R.; Wang, J. H. *Science* **1997**, *278*(5339), 838–840.
(11) Fan, H.; Lu, Y.; Stump, A.; Reed, S. T.; Baer, T.; Schunk, R.; Perez-Luna, V.; Lopez, G. P.; Brinker, C. J. *Nature* **2000**, *405* (6782), 56–60.

Published on Web 06/03/2010

that behave as independent composite hybrid species. These hybrid species are composed of oligomeric building blocks that associate with the amphiphilic component. After surfactant removal, mesoporous inorganic or hybrid thin films can be obtained.

The construction of porous materials exhibiting hierarchical structures is a particularly interesting challenge for materials chemists. Materials expressing multimodal or multiscale porosity are of major interest, particularly in catalysis, sensing, membranes, and separation-based processes where optimization of the diffusion and confinement regimes is required. As such, the design of porous materials having multimodal porosity will allow the development of innovative advanced materials with promising applications in many fields: chromatography, membranes and smart coatings, catalysis, photovoltaic and fuel cells, sensors and biosensors, etc. Recently, to fulfill the architectural requirements linked to applications of mesostructured materials as sensors, it appeared necessary to locate the mesophases on the substrate as two-dimensional (2D) arrays. Various processing techniques[12−14] have been developed with this aim. Indeed, a possible strategy to obtain hierarchically structured coatings can be achieved by combining silica−surfactant self-assembly with processing routes such as pen lithography or inkjet printing (IJP).[15−18] Previous experiments have demonstrated that the IJP process allows building of three-dimensional (3D) ceramic structures layer-by-layer, with the aid of a computer design, by depositing ceramic suspension microdroplets ejected via a nozzle.[19−23] Therefore, by using a multiprinting head device, IJP is a promising process to generate multifunctional mesoporous microdot arrays with variation of the grafted function from one dot to another. The purpose of this work is first to study the feasibility of 3D fine-scale microdot arrays of mesoporous silica by the coupling of IJP and EISA processes. In a second step, in situ functionalization of the microdots is achieved by introducing a hydrophobic agent directly into the precursor sol before printing, and the resulting hydrophobic behavior of the microdot arrays is evaluated as a function of the hydrophobic agent quantity, the surface fraction occupied by the microdots, and the surface morphology of the microdots (i.e., their roughness). The influence of this hydrophobic agent on the EISA process itself is also investigated. In a third step, one-pot bifunctionalization of the microdots by introducing a thiol precursor is studied. The influence of this supplementary function on the structural organization as well as the capability of trapping heavy metals is investigated.

Such hierarchically patterned coatings based on inorganic or hybrid structures could be used to develop hyperhydrophobic or hyperhydrophilic coatings and catalytic layers. Moreover, the possibility of using an inkjet multiprinting head system to graft by "one-pot" synthesis different organic functionalities from one dot to another opens the door to the fabrication of highly sensitive miniaturized sensors. These smart sensors would be based on multiarrays of functional mesoporous dots and could be used in many different fields (heavy-metal trapping, artificial noses, and molecular recognition applied to antibody detection for the diagnostic of infections).

Experimental Section

Different precursor solutions were tested for the fabrication of 3D silica mesoporous microdots by IJP. To be compatible with the IJP head, the solutions must be characterized by a viscosity and a surface tension ranging between 5 and 20 mPa·s and between 30 and 35 mN/m, respectively. In addition, to optimize the droplet generation, a ratio of ejection $Re/We^{1/2}$ in the adequate range (1−10) is required to minimize the pulse amplitude for ejection and to avoid satellite droplet formation. The Reynolds number (Re) and the Weber number (We) are equal to $\nu r\rho/\eta$ and $\nu^2 r\rho/\sigma$, respectively, so that the ratio of ejection is equal to $(\sigma\rho r)^{1/2}/\eta$, where ρ, η, and σ are the ink density, viscosity, and surface tension, respectively, r is the radius of the nozzle, and ν is the fluid velocity. A low vapor pressure of the solvent is needed to avoid a too fast evaporation at the nozzle aperture.

The precursor solutions were based on chemical compositions developed for the deposition of mesoporous silica films by dip coating;[24] i.e.

(i) Tetraethylorthosilicate (TEOS) was used as a polymerizable inorganic precursor.
(ii) The pH was adjusted to 1.85 by the addition of nitric acid to water with a H_2O/TEOS molar ratio fixed at 5 to favor fast hydrolysis and minimum condensation, promoting the formation of small oligomers.
(iii) Triblock copolymer Pluronic F127 (PEO_{106}−PPO_{70}−PEO_{106}) with a F127/TEOS molar ratio equal to 0.006 was used as a nonionic structuring agent.[13,14]
(iv) The solvent was ethanol: the molecular weight of the surfactant yielded a viscosity of 4.8 mPa·s for an EtOH/TEOS molar ratio of 20.

Moreover, the addition of a hydrophobic organosilane cosurfactant $R'Si(OR)_3$, i.e., $F_3C(CF_2)_5CH_2CH_2Si(OC_2H_5)_3$

(12) Yang, H.; Coombs, N.; Ozin, G. A. *Adv. Mater.* **1997**, *9*(10), 811–814.
(13) Trau, M.; Yao, N.; Kim, E.; Xia, Y.; Whitesides, G. M.; Aksay, I. A. *Nature* **1997**, *390*(6661), 674–676.
(14) Yang, P.; Deng, T.; Zhao, D.; Feng, P.; Pine, D.; Chmelka, B. F.; Whitesides, G. M.; Stucky, G. D. *Science* **1998**, *282*(5397), 2244–2246.
(15) Fan, H.; Reed, S.; Baer, T.; Schunk, R. P.; Lopez, G.; Brinker, C. J. *Microporous Mesoporous Mater.* **2001**, *44*−*45*, 625–637.
(16) Fan, H.; Lopez, G. P.; Brinker, C. J. In *Materials Research Society Symposium—Proceedings*, San Francisco, CA, 2000; Chrisey, D. B., Gamota, D. R., Helvajian, H., Taylor, D. P., Eds.; Materials Research Society: Warrendale, PA, 2000; pp 231−240.
(17) Innocenzi, P.; Kidchob, T.; Falcaro, P.; Takahashi, M. *Chem. Mater.* **2008**, *20*(3), 607–614.
(18) Mougenot, M.; Lejeune, M.; Baumard, J. F.; Boissiere, C.; Ribot, F.; Grosso, D.; Sanchez, C.; Noguera, R. *J. Am. Ceram. Soc.* **2006**, *89*(6), 1876–1882.
(19) Senlis, G.; Dubarry, M.; Lejeune, M.; Chartier, T. *Ferroelectrics* **2002**, *2002*, 279–284.
(20) Lejeune, M.; Chartier, T.; Dossou-Yovo, C.; Noguera, R. *J. Eur. Ceram. Soc.* **2009**, *29*(5), 905–911.
(21) Noguera, R.; Dossou-Yovo, C.; Lejeune, M.; Chartier, T. *J. Phys. IV: JP* **2005**, *2005*, 87–93.
(22) Noguera, R.; Dossou-Yovo, C.; Lejeune, M.; Chartier, T. *J. Phys. IV Fr.* **2005**, *126*, 5.
(23) Noguera, R.; Lejeune, M.; Chartier, T. *J. Eur. Ceram. Soc.* **2005**, *25* (12 special issue), 2055–2059.
(24) Grosso, D.; Cagnol, F.; Soler-Illia, G. J. D. A. A.; Crepaldi, E. L.; Amenitsch, H.; Brunet-Bruneau, A.; Bourgeois, A.; Sanchez, C. *Adv. Funct. Mater.* **2004**, *14*(4), 309–322.

(TFTS), to the formulation was also investigated with a TFTS/TEOS molar ratio of 5%. Because of its hydrophobic nature, TFTS addition could contribute to improving the deposit definition on hydrophilic substrates,[18] to increasing the hydrophobic nature of the microdot arrays, and to modifying the silica−surfactant self-assembly.

The aging time of the corresponding solutions was adjusted to control the size of the oligomers in order to guarantee the self-assembly of the micelles with the organic precursor during evaporation of the solvent and to avoid clogging of the printing head by formation of a gel in the nozzles. ^{29}Si NMR studies of TEOS hydrolysis for the F127 solution and with the addition of TFTS allowed one to select different aging times corresponding to mainly Q_2 [$Si(OSi)_2(OX)_2$] and Q_3 [$Si(OSi)_3(OX)$] condensed species.[18] In fact, a small size of oligomers (mainly Q_1 [$Si(OSi)(OX)_3$] species) inhibits the formation of a silica inorganic network, whereas a high degree of condensation (mainly Q_4 [$Si(OSi)_4$] species) prevents organization of the surfactant from occurring. Therefore, for the F127 solution, the aging time was fixed to 96 h. Because an increase in the condensation rate was previously observed after the addition of 5 mol % TFTS, different solutions were prepared before ejection with aging times ranging from 24 to 96 h.

The IJP equipment developed in the SPCTS laboratory is a drop-on-demand type with piezoelectric printing heads. The printing-head displacement has a resolution of 0.5 μm, a reproducibility of 2 μm, and an accuracy of 2 μm. Additional technical data are given in the corresponding patent (PCT/RF04/02150) and by the equipment manufacturer under the reference Ceraprinter L01 (Ceradrop, Ester Technopole, BP 36921, Limoges, France).

Before fabrication of the microdot arrays, the electric pulse applied to the nozzle was adjusted for each sol to get a consistent droplet ejection. This adjustment was carried out by capturing stroboscopically backlit images of the ejection with a CCD video camera. The 2D (i.e., monolayer) microdot arrays were achieved at room temperature by deposition of periodically spaced out droplets. The droplet size was adjusted to 60 μm in a first step. The 3D microdot arrays were obtained by time-delayed successive deposits of droplets on the same location to generate pillars. The delay between two successive deposits at the same location varied between 1 and 10 min. The periodic space between each microdot center was fixed between 120 and 250 μm for the 3D patterned arrays. The patterned microdot arrays were deposited on hydrophilic silicon substrates with hydroxylated native silicon oxide (SVM Inc., ref SW 150 mm/p/boron).

After fabrication, the 2D and 3D patterned arrays were heated at 130 °C for 2 days to stiffen the inorganic network through extended condensation. They were then characterized as follows: (i) the size and morphology were determined by optical microscopy, interferometric microscopy, and scanning electron microscopy (SEM) and (ii) the structure of the deposits was investigated by X-ray diffraction (XRD) in a $\theta-2\theta$ Bragg−Brentano scattering geometry, by 2D small-angle X-ray scattering (SAXS) experiments, and by transmission electronic microscopy (TEM) characterization of cross-sectioned microdots and the function efficiency by confocal scanning microscopy (CSM). Typical 3D microdot arrays are presented in Figure 1.

Moreover, the hydrophobicity of 3D microdot arrays was also characterized. In fact, in addition to the hydrophobic behavior of the organosilane TFTS added to the formulation, by deposition of microdot arrays, the IJP process allows one to create a surface roughness that can be beneficial to the hydrophobic nature of the deposits according to previous studies.[25−32] In order to evaluate the impact of the microtexture of the 3D microdot arrays on their hydrophobic behavior, different samples were achieved with variable numbers of deposited layers and variable interspaces between microdot centers. This allows one in this way to modify the microtexture of the deposits by defining, on one side, a variable roughness R of the microdot and, on the other side, a variable surface fraction F occupied by the microdots, which are respectively given by the following equations:

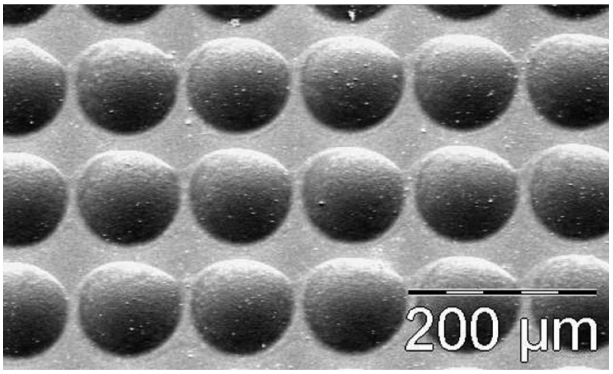

Figure 1. SEM image of a 25-layer microdot array.

$$R = 1 + h^2/r_c{}^2 \quad (1)$$

where r_c is the dome radius and h its height.

$$F = Rf_1/(Rf_1 + f_2) \quad (2)$$

where f_1 is the projected surface fraction occupied by microdots, f_2 is the surface fraction of the substrate not covered by microdots, and R is the roughness calculated from eq 1.

Results and Discussion

The first challenge of our work consisted of adapting the formulation of the initial sol to fulfill the requirements of both the material and the shaping technique, knowing that these requirements could be contradictory. A compromise had then to be found to get an optimized ejection (no clogging of the nozzle aperture) and a good structuration of the mesoporous network. In this compromise, the addition of the hydrophobic organosilane, TFTS, played a key role. Indeed, adjustment of the process parameters and TFTS, i.e., the coupling of chemistry and processing, allows one to notably improve the large-scale organization of the mesoporosity.

1. Influence of the Aging Time of the Initial Solutions. The influence of the hydrophobic organosilane TFTS addition (with a TFTS/SiO_2 molar ratio of 5%) on the condensation rate of the two sols, with and without TFTS, were previously studied at different aging times by ^{29}Si NMR liquid analyses.[18] These have revealed a

(25) Yoshimitsu, Z.; Nakajima, A.; Watanabe, T.; Hashimoto, K. *Langmuir* **2002**, *18*(15), 5818–5822.
(26) Patankar, N. A. *Langmuir* **2003**, *19*(4), 1249–1253.
(27) Shibuichi, S.; Onda, T.; Satoh, N.; Tsujii, K. *J. Phys. Chem.* **1996**, *100*(50), 19512–19517.
(28) Callies, M.; Chen, Y.; Marty, F.; Pépin, A.; Quére, D. *Microelectron. Eng.* **2005**, *78−79*(1−4), 100–105.
(29) Patankar, N. A. *Langmuir* **2004**, *20*(19), 8209–8213.
(30) He, B.; Patankar, N. A.; Lee, J. *Langmuir* **2003**, *19*(12), 4999–5003.
(31) Öner, D.; McCarthy, T. J. *Langmuir* **2000**, *16*(20), 7777–7782.
(32) Quéré, D. *Nat. Mater.* **2002**, *1*(1), 14–15.

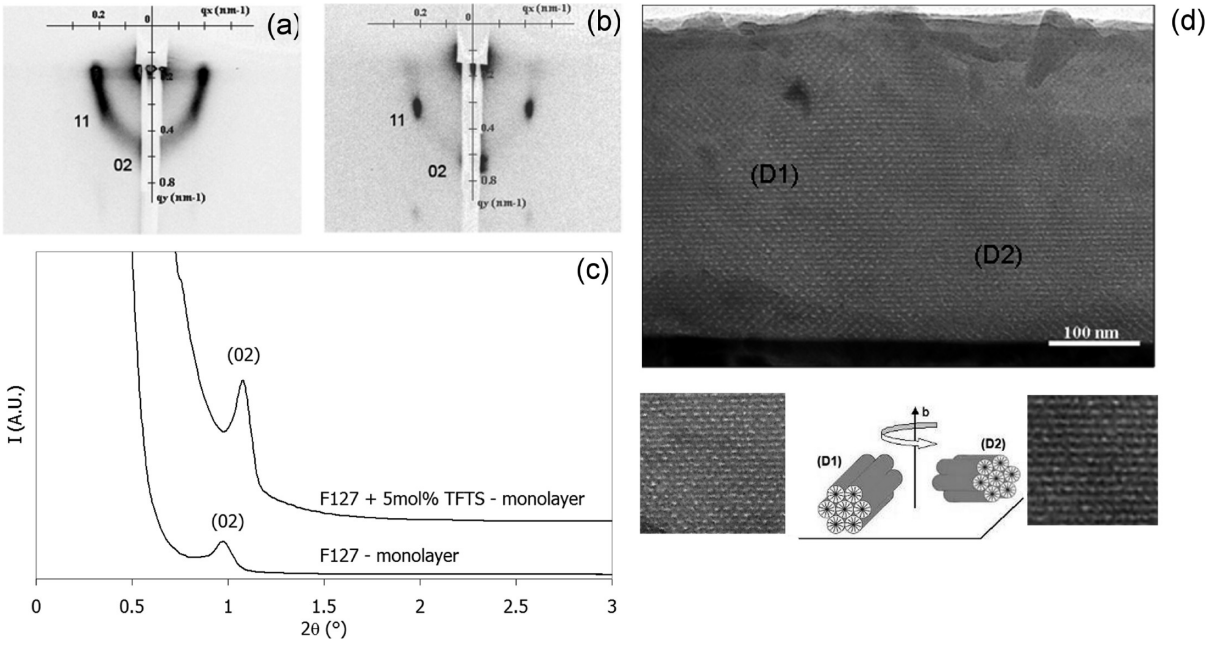

Figure 2. Structural organization of the monolayer microdot arrays made by IJP: 2D SAXS patterns of monolayer microdot arrays made from a F127 solution without (a) and with (b) 5 mol % TFTS addition for an initial aging time of 96 h (postheating treatment at 130 °C for 2 days); (c) XRD diagrams of the same microdot arrays realized from a solution with and without TFTS; (d) TEM micrograph of a cross section of one microdot made with a 5 mol % TFTS solution.

beneficial effect of TFTS on the condensation rate at the early stage by showing a higher amount of Q_3 species in the solutions containing TFTS. However, for longer aging times (96 h and more), the condensation rates become similar with and without TFTS.

2. Study of the Structural Organization of Monolayer Microdot Arrays of Silica Functionalized by TFTS. At the nanoscale, GISAXS characterizations (Figure 2) of deposited monolayer microdot arrays allow one to reveal the mesostructure organization. Sharp diffraction spots are mainly observed in the presence of TFTS, which indicates a preferential orientation of organized domains parallel to the substrate (Figure 2b). On the opposite side, both a diffraction ring and diffraction spots are observed without TFTS (Figure 2a). This signature is attributed to the coexistence of mesostructured domains presenting random orientations with respect to the surface.

The positive effect of TFTS for the alignment of cylindrical pores parallel to the surface is confirmed by TEM observations (Figure 2d). Each monolayer microdot exhibits in its whole thickness (i.e., about 350 nm) a structural organization corresponding to a centered rectangular structure with cylindrical micelles parallel to the substrate surface. This structure results from the shrinkage of a 2D hexagonal arrangement of the micellar cylinders in a direction perpendicular to the substrate. This shrinkage occurs during thermal treatment at 130 °C, as mentioned in a previous work.[33] It must also be noticed that deposits exhibit structured domains (D1 and D2) differently oriented around an axis perpendicular to the substrate surface.

XRD can be used to characterize the centered rectangular structure. Indeed, a single peak is observed for microdots made with sols with or without TFTS (Figure 2c). This peak corresponds to the plane (02) of the centered rectangular structure parallel to the substrate.[34]

In the presence of TFTS, it is translated toward a higher angle ($2\theta_{max}$ = 0.98° without TFTS against 1.08° with TFTS), which corresponds respectively to a decrease of the b parameter from 18 to 16.3 nm, i.e., to a lattice contraction of 9% perpendicularly to the 02 direction.

This decrease of the d_{02} distance is assumed to be due to chemical interactions of TFTS with the other entities of the system. Although it still has to be clarified, we assume that TFTS could behave as a kind of cosurfactant: it would locate its hydrophilic head $Si(OC_2H_5)_x(OH)_{3-x}$ close to silica oligomers, where it could be incorporated in the network by cocondensation, locating its hydrophobic group at the pore surface (Figure 3). Moreover, previous works[35] relative to the effect of the addition of an organosilane with long chains, such as TFTS, to an F127-based solution have revealed that this one could interact with the hydrophobic block of the surfactant F127. This interaction could induce an additional structural shrinkage, together with that resulting from thermal treatment at 130 °C as was already explained (Figure 2c).

The improvement of the deposit global organization, when achieved from a 5 mol % TFTS formulation, would

(33) Klotz, M.; Albouy, P. A.; Ayral, A.; Menager, C.; Grosso, D.; Van der Lee, A.; Cabuil, V.; Babonneau, F.; Guizard, C. *Chem. Mater.* **2000**, *12*(6), 1721–1728.

(34) Falcaro, P.; Grosso, D.; Amenitsch, H.; Innocenzi, P. *J. Phys. Chem. B* **2004**, *108*(30), 10942–10948.

(35) Matheron, M. *Films mésoporeux hybrides organiques-inorganiques: synthèse, organisation des pores et application en optique ophtalmique*; Thesis Ecole Polytechnique: Palaiseau, France, 2005.

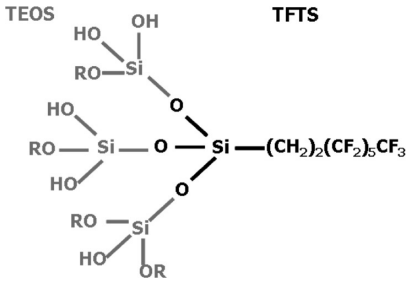

Figure 3. Possible mechanism of interaction between TEOS and TFTS.

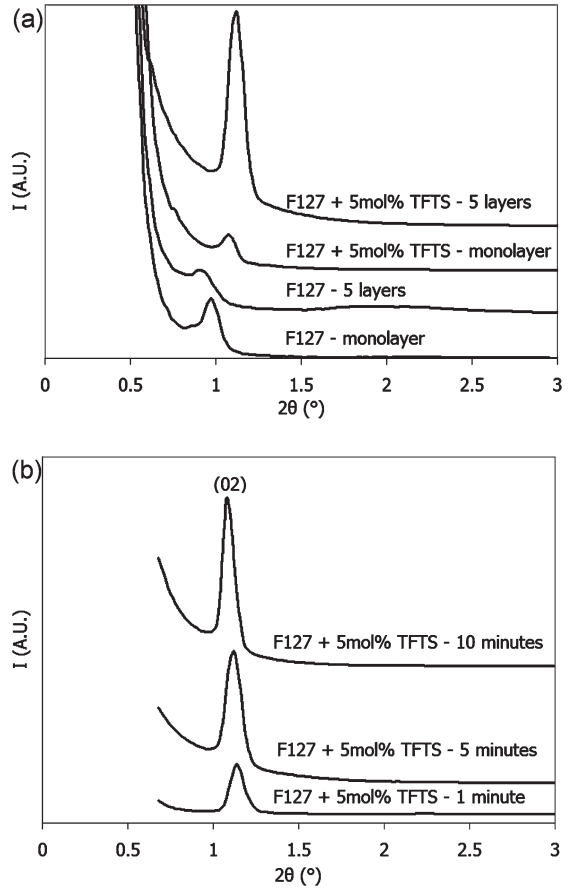

Figure 4. 1D XRD diagrams of (a) microdots made of different numbers of layers from a solution without and with 5 mol % TFTS initially aged for 96 h (drying time between each layer equal to 5 min and postheating treatment at 130 °C for 2 days) and (b) microdots made of five layers from a solution with 5 mol % TFTS initially aged for 96 h for drying times between each layer ranging from 1 to 10 min (postheating treatment at 130 °C for 2 days).

result in a decrease of the time necessary for the structural organization of the deposit to proceed. The fact that TFTS would behave as a fluorocarbon surfactant with the silica oligomers could also explain why the final mesopore organization is enhanced with TFTS addition in the initial sol formulation. Indeed, TFTS, which is partially miscible[36] with a hydrocarbon surfactant, formed with the silica oligomers some nucleation seeds, which accelerate the self-assembly step and structural organization of the microdots at the early stage of drying after ejection. Then, for a fixed drying time (i.e., rigidification time), the shorter the self-assembly time, the longer the time remaining for micelle alignment with air and substrate interfaces.

(36) Han, Y.; Ying, J. Y. *Angew. Chem., Int. Ed.* **2005**, *44*(2), 288–292.

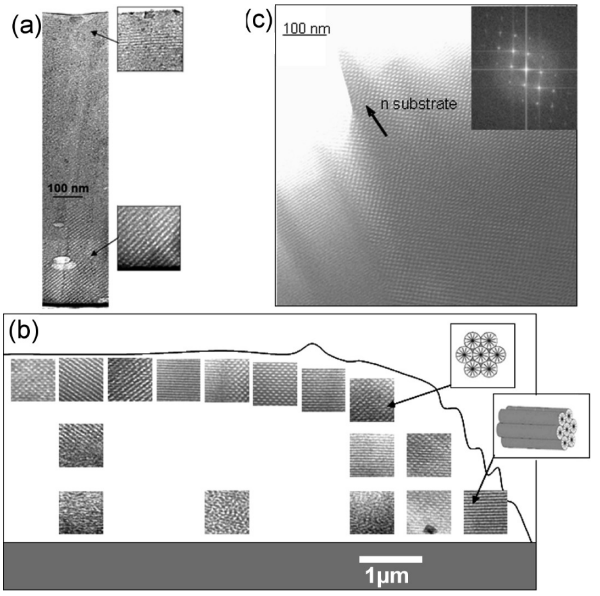

Figure 5. TEM micrographs of a cross section of a microdot of five layers made with a 5 mol % TFTS solution aged for 96 h: (a) for a drying time of 1 min between two successive layers; (b) for a drying time of 10 min; (c) for a drying time of 10 min showing a centered rectangular structure at the surface of the microdot.

3. Characterization of the Structural Organization of Multilayer Microdot Arrays. *a. Effect of TFTS Addition on the Structural Organization.* XRD characterizations in a $\theta-2\theta$ Bragg−Brentano scattering geometry help one to understand what happens to the mesoporosity organization when several layers are stacked. In the absence of TFTS (Figure 4a), a significant degradation of the organization is observed with an increase of the number of layers. This effect is due to the inflow of solvent between successive depositions. On the contrary, with TFTS addition (Figure 4a), each layer presents a better final structural organization and the bottom layers become less sensitive to degradation by postdeposition, as pointed out by the significant diffraction peak observed.

b. Effect of the Drying Time between Two Successive Layers. XRD characterizations (Figure 4b) of microdots, made from TFTS formulations and the superposition of five layers, reveal that the mesostructure organization is improved by increasing the drying time between two successive layers.

Indeed, for short drying times such as 1 min, TEM images show that only the interfaces exhibit a mesostructure organization (Figure 5a). Because of the very short drying time, everything happens a bit as if only one single and massive droplet was formed. As a result, the mesostructure organization occurs only close to the outer surface of the global deposit, near the interface with air, before droplet rigidification. On the opposite side, the internal part tends to exhibit a wormlike structure (Figure 5a).

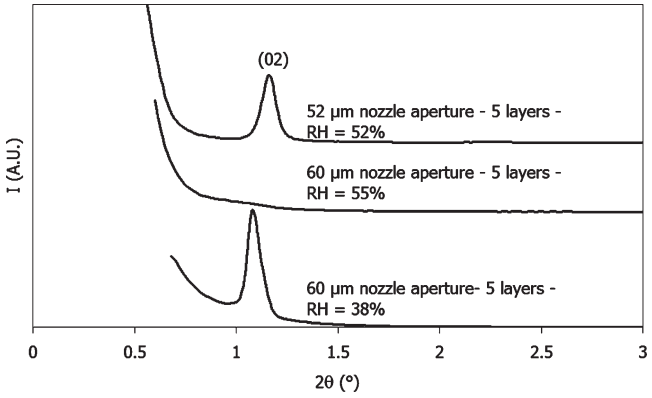

Figure 6. XRD diagrams of microdot arrays made of five layers (drying time between successive layers = 10 min) fabricated from 5 mol % TFTS formulations aged for 96 h and ejected at different ambient RHs and with different nozzle aperture diameters.

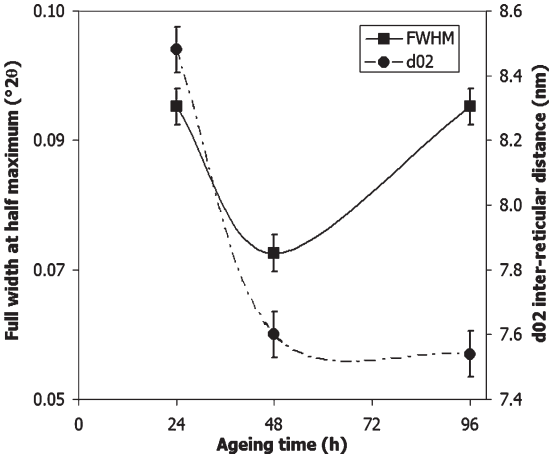

Figure 7. Evolution of the fwhm of XRD peaks and their corresponding d_{02} inter-reticular distances as a function of the aging times for microdot arrays made of 25 layers (10 min of drying time) and fabricated using a 52 μm nozzle aperture with 5 mol % TFTS formulations (postheating at 130 °C for 2 days).

For longer drying times (10 min), well-organized domains are observed within a 1.5 μm depth from the air/deposit interface (Figure 5b). As found for monolayer deposits, the structural organization corresponds to a centered rectangular structure. The revolution axes of cylindrical micelles are aligned in a plane parallel to the substrate, with different orientations leading to the previously mentioned domains.

Moreover, Figure 5c reveals that the deposit can exhibit a single orientation on a large scale (up to a few hundred nanometers), i.e., corresponding to different deposited layers.

c. Effect of the Decrease of the Droplet Volume. In order to decrease the inflow of solvent that contributes to the destruction of the structural organization of the bottom layers, it is possible to reduce the droplet volume. This one was reduced from 100 to 35 pL by using a 52 μm nozzle aperture instead of the initial 60 μm nozzle aperture.

The XRD diagram (Figure 6) of a five-layer deposit prepared with a 5 mol % TFTS formulation ejected through the 52 μm nozzle aperture shows indeed a very good structural organization, which confirms that the decrease of the deposited volume avoids the solvent accumulation and greatly limits the degradation of the structure.

Furthermore, a comparison of the XRD diagrams (Figure 6) performed on microdot arrays made from 5 mol % TFTS formulations ejected for a similar humidity [around 55% relative humidity (RH)] through the 52 and 60 μm nozzle apertures shows that a decrease of the droplet volume makes the mesostructural organization much less sensitive to RH variations.

d. Adjustment of the Aging Time of the Sol. Until now, the aging time was arbitrarily fixed at 96 h considering

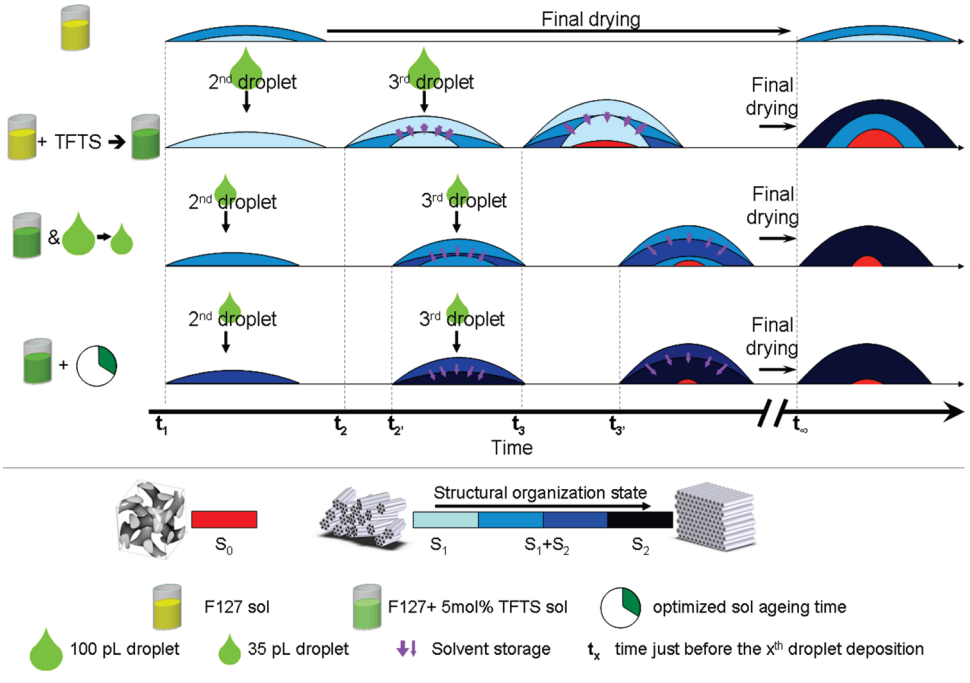

Figure 8. Scheme of the evolution of the structural organization of a microdot during deposition and the strategy of improvement.

Table 1. Radius, Height, and Roughness (Calculated Using eq 1) of the Deposits and the Estimated Contact Angle of a Water Droplet on a Substrate Entirely Covered by Microdots ($F = 1$) Made from 5 mol % TFTS Formulations Aged for 48 h as a Function of the Number of Layers

no. of layers	microdot radius r_c (μm)	microdot height h (μm)	roughness R	estimated contact angle for $F = 1$ (deg)
1	51	0.1	1.000 006 04	118
5	58	1.1	1.000 331 99	125
25	61	4.4	1.005 200 01	131

previous works on similar materials.[33,37] Some microdot arrays of 25 layers were realized using the 52 μm nozzle aperture (10 min of drying time) for different aging times of the sol before ejection. Then, they were analyzed by XRD.

The lowest full width at half-maximum (fwhm) of the 02 peak is obtained for an aging time of 48 h (Figure 7). Hence, this aging time gives the best organization degree of the deposits. The d_{02} inter-reticular distance (Figure 7) decreases from 8.5 to 7.6 nm because of condensation of the sol. Above 48 h, the d_{02} distance becomes invariant.

When the condensation time of the sol is too low (24 h), the oligomers are very small and they cannot correctly percolate around the surfactant micelles,[38] so that the structural organization of the deposit is bad (high fwhm). Conversely, if the condensation time is too long (96 h), the clusters of silica oligomers are too big and can deform the micellar structure.

In conclusion, Figure 8 summarizes the different strategies used to improve the structural organization of the mesoporous silica microdots.

4. Hydrophobic Behavior of Microdot Arrays Made from 5 mol % TFTS Formulations. For the different 3D microdot arrays achieved with variable numbers of deposited layers and variable interspaces between microdot centers, the corresponding roughness (R) and surface fraction (F) were determined respectively according to eqs 1 and 2 mentioned in the Experimental Section.

Then, for each sample, the contact angle (θ^*) of a water droplet of 2.5 μL was measured and reported as a function of the surface fraction (F) for three different roughnesses (Figure 9a).

The experimental results exhibit a linear behavior for each number of layers (i.e., for each roughness R), which converges to the same initial point ($F = 0$). Therefore, these can be analyzed by using a combination of the Cassie[39] and Wenzel[40] laws as follows:

$$\cos \theta^* = FR \cos \theta_{\text{dots}} + (1 - F) \cos \theta_{\text{substrate}} \qquad (3)$$

where θ^* is the apparent contact angle of a liquid on the surface formed of mesoporous silica microdots deposited on a native silica substrate, F is the surface fraction corresponding to the mesoporous silica microdots, R is the roughness of the microdot arrays, θ_{dots} is the contact angle of a liquid on a surface totally covered by mesoporous silica, and $\theta_{\text{substrate}}$ is the contact angle of a liquid on the substrate without microdots.

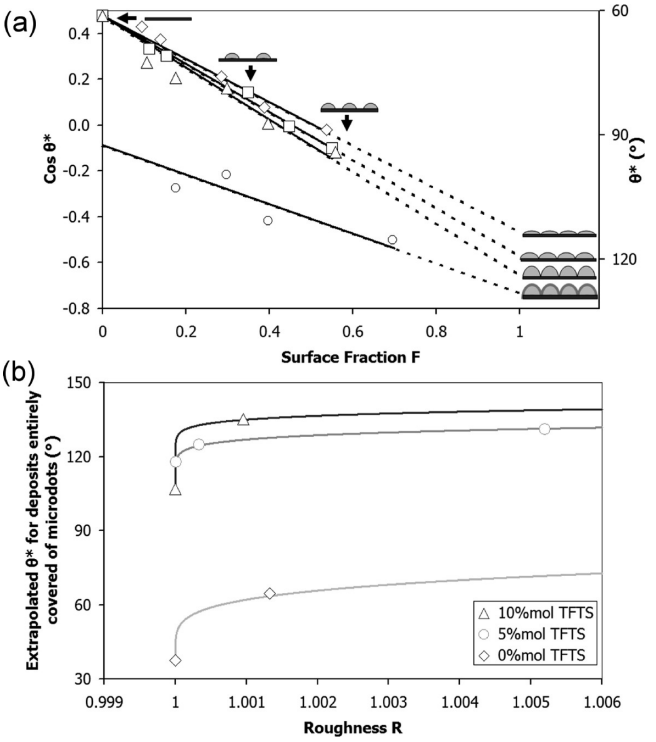

Figure 9. (a) Evolution of the contact angle θ^* according to the surface fraction occupied by microdots made with a drying time of 1 min using a 52 μm nozzle aperture from 5 mol % TFTS formulations aged for 48 h for 1 (◇), 5 (□), and 25 layers [before (△) and after (○) TFTS postgrafting] and (b) evolution of the estimated contact angle of a water droplet on a substrate entirely covered by microdots ($F = 1$) as a function of the roughness R (defined using eq 1) for 0 (◇), 5 (○), and 10 (△) mol % TFTS in the sol formulation.

Therefore, the same initial point ($F = 0$) corresponds to a water droplet on a bare substrate, here 61°.

Moreover, from this linear fit, it is possible to extrapolate the contact angle θ^* for a surface fraction of microdots equal to 1 (i.e., microdots entirely covering the substrate; Table 1.).

Despite the weak variation of the roughness, the contact angle notably increases with this one. Some authors[26] reported a contact angle of 138° for a roughness of 1.1 obtained by machining of the hydrophobic surfaces of fluorinated compounds. By comparison, for a lower roughness of 1.005, 5 mol % TFTS-based deposits fabricated by IJP exhibit a contact angle of 131°.

The presence of the silica substrate between the microdots can limit the hydrophobic properties of the samples fabricated by IJP. In order to compare our results with other studies for which the entire surface was hydrophobic,[25,28,41] 25-layer patterned substrates were coated with TFTS by postgrafting it in a vapor phase.

(37) Wanka, G.; Hoffmann, H.; Ulbricht, W. *Macromolecules* **1994**, *27* (15), 4145–4159.
(38) Besson, S. *Films organisés de silice mésoporeuse: synthèse, caractérisation structurale et utilisation pour la croissance de nanoparticules'*; Thesis Ecole Polytechnique: Palaiseau, France, 2002.
(39) Cassie, A. B. D.; Baxter, S. *Trans. Faraday Soc.* **1944**, *40*, 546–551.
(40) Wenzel, R. *Ind. Eng. Chem.* **1936**, No. 28, 8.
(41) Soresi, B.; Quartarone, E.; Mustarelli, P.; Magistris, A.; Chiodelli, G. *Solid State Ionics* **2004**, *166*(3−4), 383–389.

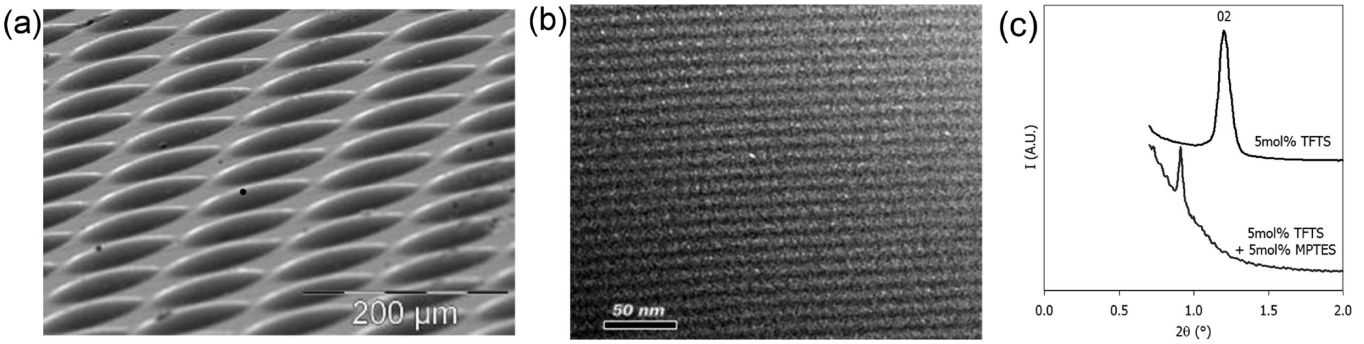

Figure 10. (a) SEM images of 25-layer microdot arrays realized from a sol aged 48 h and in situ functionalized with 5 mol % MPTES and 5 mol % TFTS. (b) TEM micrograph of a cross-sectioned 25-layer microdot realized from a sol aged 48 h and in situ functionalized with 5 mol % MPTES and 5 mol % TFTS. (c) XRD diagrams of two 25-layer samples functionalized or not with 5 mol % MPTES achieved with sols aged 48 h (drying time between two successive layers equal to 1 min and postheating treatment for 2 days at 130 °C).

Figure 9a shows that grafting of TFTS on the surface of the microdot arrays improves their hydrophobic properties. As expected, this improvement is more significant for the low surface fractions of microdots. For a surface fraction of microdots equal to 1, the extrapolated improvement is negligible, revealing the high effectiveness of the in situ functionalization by 5 mol % TFTS.

It would mean that for 5 mol % TFTS the surface of the dots is almost saturated with TFTS. To validate this hypothesis, the hydrophobicity of deposits made with 10 mol % TFTS was studied. In order to be only dependent on the quantity of TFTS, we considered the contact angle θ^* of a water droplet on a substrate entirely covered by microdots ($F = 1$). This contact angle was extrapolated by linear fitting of experimental data.

The values in Figure 9b corresponding to a roughness equal to 1 were obtained on deposits made by spin coating of the same sol formulation as that used for IJP.

For 10 mol % TFTS, variation of the contact angle is low, only 6% of the absolute value in comparison to what is measured for 5 mol % TFTS, confirming that saturation of the surface by TFTS is almost reached from 5 mol % TFTS in the initial sol formulation (Figure 9b).

Alternatives to further improving the hydrophobicity of the deposits could be to change the hydrophobic organosilane or to increase the roughness (the number of layers),

Therefore, in conclusion, this part of the study underlines how the IJP process is a very flexible manner in which to adjust the contact angle to a given value according to the aimed application.

5. One-Pot Bifunctionalization of Microdot Arrays with TFTS and a Thiol Group. For this study, the thiol function is introduced under the form of (3-mercaptopropyl)-triethoxysilane [MPTES, $HSC_3H_6Si(OC_2H_5)_3$]. The addition of TFTS is still needed to allow a good ejection of this sol regarding the IJP process parameters. The addition of MPTES in the solution is performed in one pot with the fluorinated organosilane: the tested formulation contains 5 mol % TFTS and 5 mol % MPTES.

Optimization of the aging time before ejection is performed using the same protocol as that used for the formulation including only TFTS.

Figure 10a shows the morphology of 25-layer, 120 μm spaced microdot arrays realized from the sol aged for 48 h: the microdots correspond to domes with a diameter of 110 μm and a height of 7.5 μm.

An XRD analysis allows one to check the mesostructuration of these microdots (Figure 10c). Both materials with or without MPTES are quite well organized, but there is a significant increase of the cell parameter because of a lamellar structure parallel to the substrate when the thiol function is used in combination with TFTS (Figure 10b).

Previous works[42] have shown that it is possible to examine the mesoporosity accessibility in regular circular patterns by impregnation of a fluorescent dye. We chose to use a Rhodamine B dye, which should diffuse in the porosity.

For this purpose, a five-layer microdot array, achieved from the sol only functionalized with TFTS aged 48 h with 52 μm nozzles with a drying time of 10 min between two successive layers, was thermally treated at 240 °C for 2 h in order to remove the surfactant and later impregnated for 2 h in an ethanolic solution of 1 μmol/L Rhodamine B. As a result, laser CSM images show red fluorescent dots with feature sizes (Figure 11a) corresponding more or less to the size of inkjet-printed dots. The dark background indicates that the Rhodamine B dye does not interact with the silica surface itself. The results (Figure 11b) are similar in the case of the same microdots bifunctionalized by TFTS and thiol functions and also impregnated for 2 h with the dye. The two above-mentioned preliminary experiments demonstrate the accessibility of the mesoporous structures to Rhodamine B in both cases.

Then we further impregnate for 12 h the same kinds of samples with 3.5 and 17 nm gold nanoparticle (GNP) suspensions (1 mmol/L) in water elaborated upon in the work of Jana et al.[43] As a consequence, we observe a quenching of fluorescence. With 3.5 nm GNP, this quenching is higher when the samples are bifunctionalized (Figure 11f). Such a result indicates that the thiol

(42) Chen, H. T.; Crosby, T. A.; Park, M. H.; Nagarajan, S.; Rotello, V. M.; Watkins, J. J. *J. Mater. Chem.* **2009**, *19*(1), 70–74.
(43) Jana, N. R.; Gearheart, L.; Murphy, C. J. *Langmuir* **2001**, *17*(22), 6782–6786.

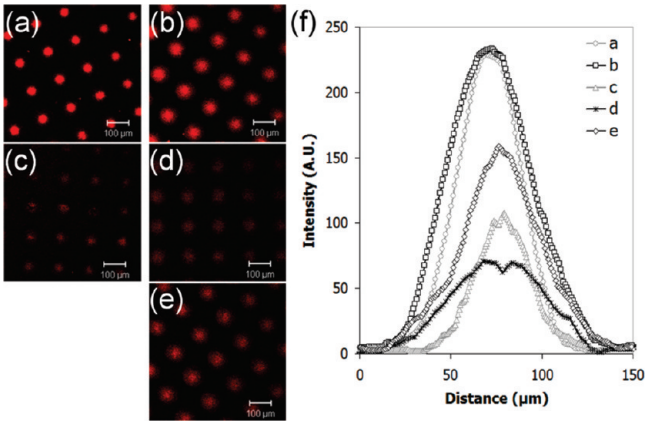

Figure 11. Fluorescence images of five-layer microdot arrays achieved with 52 μm nozzles from the sol aged 48 h with a drying time of 10 min between two successive layers and thermally treated at 240 °C for 2 h in order to remove the surfactant: (a) only functionalized with TFTS and impregnated with Rhodamine B; (b) bifunctionalized with TFTS and MPTES and impregnated with Rhodamine B; (c) only functionalized with TFTS and impregnated in Rhodamine B and then with a 3.5 nm GNP suspension; (d) bifunctionalized with TFTS and MPTES and impregnated with Rhodamine B and then with a 3.5 nm GNP suspension; (e) bifunctionalized with TFTS and MPTES and impregnated with Rhodamine B and then with a 17 nm GNP suspension. (f) Comparison of the fluorescence intensity profiles of mesoporous silica microdots (a−e).

groups preferentially trap chemically the GNP, initially in a suspension in water, despite the presence of the hydrophobic organosilane.

For impregnation with 17 nm GNP, the quenching of fluorescence (Figure 11f) is lower than that observed with 3.5 nm GNP. In that case, the 17 nm GNP cannot be chemically trapped in the bulk of the material because that they simply cannot physically access that bulk knowing that the size of the mesopore is on the order of 6 nm.

Conclusions

Thanks to numerous investigation techniques such as SAXS, TEM, and CSM, this work highlights the feasibility of one-pot multifunctionalization of well-structured patterned silica microdot arrays with both TFTS CF_3-$(CF_2)_5CH_2CH_2Si(OC_2H_5)_3$ and thiol functionalities $HSCH_2CH_2CH_2Si(OC_2H_5)_3$, emphasizing the wide range of accessible nanostructured porous hybrid materials that result from the coupling of IJP and EISA.

Indeed, mesostructured silica microdot arrays were successfully deposited by IJP from precursor solutions containing a partially hydrolyzed TEOS with a nonionic surfactant, Pluronic F127 ($PEO_{106}-PPO_{70}-PEO_{106}$). Thanks to the addition in the initial sol of a hydrophobic organosilane TFTS, the structural organization of mesoporous monolayers shaped by IJP as microdot arrays was notably improved by promoting the coassembly of surfactant and silica species. Moreover, very well-structured 3D microdot arrays (25 stacked layers) were obtained by adjusting IJP processing parameters (i.e., drying time between two successive layers and the droplet size) and by controlling the aging time of the sol before deposition.

The hydrophobic behavior of TFTS was also exploited to produce superhydrophobic surfaces, controlling at the same time the roughness by IJP. In fact, a one-pot functionalization with a low TFTS content (5 mol %) allows one to reach a contact angle of 131° of a water droplet on a microdot array, entirely covering the silicon substrate, which corresponds to a roughness of 1.005.

The feasibility of a one-pot bifunctionalization with both TFTS and thiol groups was also demonstrated. The capability of chemically trapping GNPs (3.5 nm) in the porosity of bifunctionalized microdots was then clearly established thanks to CSM characterizations.

The possibility of using an inkjet multiprinting head system to graft in "one pot" different functions from one dot to another opens the door to fabrication by the coupling of IJP to EISA of highly sensitive miniaturized sensors. These sensors could be used in different fields such as heavy metal trapping, artificial noses, and molecular recognition applied to antibody detection for the diagnostic of infections.

Acknowledgment. This work is carried out in the framework of the FAME Network of Excellence, funded by the European Union and supported by CNRS.